
Constraints on Pulsed Emission Model for Repeating FRB 121102

Shota KISAKA ^{1,*}, Teruaki ENOTO ^{2,3}, and Shinpei SHIBATA ⁴

¹Department of Physics and Mathematics, Aoyama Gakuin University, Sagamihara, Kanagawa, 252-5258, Japan

²The Hakubi Center for Advanced Research, Kyoto University, Kyoto 606-8302, Japan

³Department of Astronomy, Kyoto University, Kitashirakawa-Oiwakecho, Sakyo-ku, Kyoto, 606-8502, Japan

⁴Department of Physics, Yamagata University, Kojirakawa, Yamagata, 990-8560, Japan

*E-mail: kisaka@phys.aoyama.ac.jp

Received (reception date); Accepted (acceptation date)

Abstract

Recent localization of the repeating Fast Radio Burst (FRB) 121102 revealed the distance of its host galaxy and luminosities of the bursts. We investigated constraints on the young neutron star (NS) model, that (a) the FRB intrinsic luminosity is supported by the spin-down energy, and (b) the FRB duration is shorter than the NS rotation period. In the case of a circular cone emission geometry, conditions (a) and (b) determine the NS parameters within very small ranges, compared with that from only condition (a) discussed in previous works. Anisotropy of the pulsed emission does not affect the area of the allowed parameter region by virtue of condition (b). The determined parameters are consistent with those independently limited by the properties of the possible persistent radio counterpart and the circumburst environments such as surrounding materials. Since the NS in the allowed parameter region is older than the spin-down timescale, the hypothetical GRP-like model expects a rapid radio flux decay of $\lesssim 1$ Jy within a few years as the spin-down luminosity decreases. The continuous monitoring will give a hint of discrimination of the models. If no flux evolution will be seen, we need to consider an alternative model, e.g., the magnetically powered flare.

Key words: key word₁ — key word₂ — ... — key word_n

1 INTRODUCTION

Among fast radio bursts (FRBs), which are radio transients with duration of milliseconds and large dispersion measure (DM) compared with expected for propagation through the Galaxy (e.g., Lorimer et al. 2007; Thornton et al. 2013), FRB 121102 was identified as a repeating source (Spitler et al. 2016). In observations over 2012-2016, 30 bursts were reported from FRB 121102 at 1.1 – 3.5 GHz with the same $DM \sim 560 \text{ cm}^{-3} \text{ pc}$ (Spitler et al. 2014; Spitler et al. 2016; Scholz et al. 2016; Chatterjee et al. 2017; Marcote et al. 2017). The flux density was $\sim 0.02 - 3.72 \text{ Jy}$, and no temporal evolution of the flux was apparently seen (Marcote et al. 2017). The Gaussian FWHM pulse width was 2.8 – 8.7 ms (Spitler et al. 2016). Since no scattering tail was observed in the pulses, the observed width would be the intrinsic width of the emission (Scholz et al. 2016).

Owing to interferometric imaging with the Karl G. Jansky Very Large Array (VLA) and European VLBI Network (EVN) observations, FRB 121102 was recently localized to $\sim 100 \text{ mas}$ and $\sim 2 - 4 \text{ mas}$ precisions (Chatterjee et al. 2017; Marcote et al. 2017). The radio observations also detected a persistent radio source with an angular separation from the bursts $\lesssim 40 \text{ pc}$ (Marcote et al. 2017). Optical observations identified the host galaxy at a redshift $z = 0.19273(8)$, corresponding to a luminosity distance of 972 Mpc (Tendulkar et al. 2017). The measured distance gives the luminosity of FRB 121102, $L_{\text{FRB}} \sim (0.03 - 6) \times 10^{42} \text{ erg s}^{-1}$ (Marcote et al. 2017).

Repetition of a FRB rules out the catastrophic origin. Although magnetically-powered flares from a highly magnetized neutron star (NS) have been suggested as candidate FRB sources (e.g., Popov & Postnov 2010; Lyubarsky 2014; Katz 2016a), significant constraints on FRB-like radio bursts during the giant flare were given by Tendulkar et al. (2016). The giant radio pulse (GRP) like emission from a young, energetic pulsar have also been suggested as an origin of the repeating FRB (e.g., Cordes & Wasserman 2016; Katz 2016a; Katz 2016b; Katz 2017a; Katz 2017b; Lyutikov et al. 2016; Lyutikov 2017). The broad distribution of the spectral index and the pulse width in FRB 121102 at $\sim 1.4 \text{ GHz}$ has been observed in the GRPs from the Crab pulsar (Karuppusamy et al. 2010; Mikami et al. 2016).

For the rotation-powered model, the observed FRB luminosity has to be lower than the spin-down luminosity. This constraint gives the allowed range of the NS parameters, the dipole magnetic

field $\sim 10^{12} - 10^{14}$ G and the rotation period $\lesssim 10$ ms (e.g., Lyutikov 2017; Metzger et al. 2017; Kashiyama & Murase 2017), although an efficient conversion mechanism to the radio emission is required as discussed in Cordes & Wasserman (2016). If the beam fraction is much lower than unity, the allowed parameter region becomes much large (Katz 2017a).

Different from thermal phenomena, non-thermal emission from pulsars should have both on- and off-pulse phases in a rotation period. The non-thermal emissions are produced during particle acceleration and creation in some limited regions in the magnetosphere such as polar cap (e.g., Daugherty & Harding 1982), outer gap (e.g., Cheng et al. 1986) and current sheet models (e.g., Kirk et al. 2002). Some complex profile structures seen in FRB pulses may reflect the non-uniform distribution of emissivity (Spitler et al. 2016; Tendulkar et al. 2017). Coherent radio pulsed emission from pulsars such as GRP is also non-thermal emission (e.g., Cordes & Wasserman 2016). Hence, in GRP-like emission model, the pulse width of FRBs gives the lower limit on the rotation period.

In this paper, we consider the GRP-like pulsed emission model for the repeating FRB 121102. In section 2, we give the constraints on the spin-down luminosity and the rotation period from the observed luminosity and the pulse width, respectively. Two conditions give stringent limit on the allowed parameter range for an NS. We also discuss prediction for the flux evolution, the constraints from the propagation effects, and possible NS formation scenarios for the source of FRB 121102 in section 3.

2 CONSTRAINTS ON GRP-LIKE EMISSION MODEL

We consider the GRP-like emission model where the emission comes from the pulsar magnetosphere. For the emission geometry, we assume a circular cone with angular width $\propto \sqrt{f_\Omega}$ as widely considered for the radio emission (e.g., Rankin 1993), where $f_\Omega (\leq 1)$ is the beaming fraction. We use fiducial radius and moment of inertia of an NS at $R_{\text{ns}} = 12$ km, and $I \sim 1.4 \times 10^{45}$ g cm², respectively. Since we focus on a very young NS whose age ($\ll 10^3$ yr) is much shorter than the decay timescales of dipole magnetic field in interior of an NS (e.g., Goldreich & Reisenegger 1992), we neglect the temporal evolution of the dipole field.

The propagation effects on the radio emission and the possible association of persistent radio source could give significant constraints on the model for FRB 121102 (Metzger et al. 2017; Lyutikov 2017; Kashiyama & Murase 2017; Cao et al. 2017; Dai et al. 2017). For example, if the injected energy from an NS changes the dynamics of surrounded materials, the observed DM could give constraints on the NS parameters. This NS nebula model gives the constraints on the NS properties as the dipole field $\sim 10^{13} - 10^{14}$ G, the initial rotation period \sim a few ms, and the age $\lesssim 10^2$ yr (Metzger

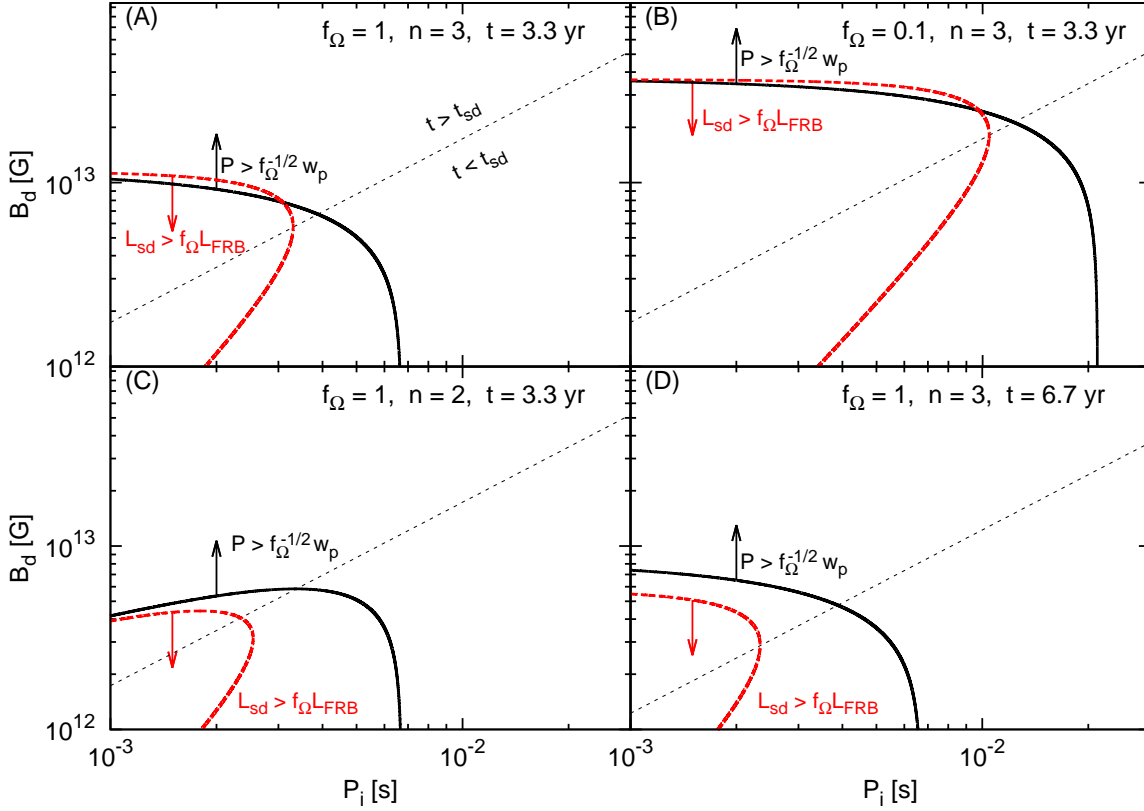


Fig. 1. Constraints on the parameter space P_i and B_d of GRP-like emission model for FRB 121102. Panel (A); fiducial case with isotropic emission ($f_\Omega = 1$), dipole spin-down formula ($n = 3$) and the lower bound of the age ($t = 3.3$ yr). We use the observed values $L_{\text{FRB}} = 6 \times 10^{42}$ erg s $^{-1}$ and $w_p = 8.0$ ms/($1 + z$) = 6.7 ms. The red thick dashed lines indicate the luminosity constraints (equation 1). The black thick solid lines indicate the pulse width constraints (equation 6). The thin dotted lines indicates the relation $t = t_{\text{sd}}$. Panel (B); anisotropic emission case ($f_\Omega = 0.1$). Panel (C); low braking index case ($n = 2$). Panel (D); older age of the NS ($t = 6.7$ yr).

et al. 2017; Lyutikov 2017; Kashiyama & Murase 2017; Cao et al. 2017; Dai et al. 2017). However, the DM is highly sensitive to the unknown ejecta properties such as non-uniformity, composition, and ionization state of circumburst materials. The detected persistent radio source could be interpreted by a low-luminosity AGN (Park et al. 2017; Marcote et al. 2017), so that the persistent source may not be directly related to the FRB source. Therefore, we only use the two observed characteristic parameters of the FRB source, the isotropic luminosity and the pulse width, to constrain on GRP-like emission model in this section.

We consider two conditions to produce the repeating FRB 121102 via GRP-like emission model. First, the spin-down luminosity L_{sd} has to be larger than the FRB intrinsic luminosity¹ (e.g.,

¹ In principle, the luminosity of sporadic emissions could exceed the spin-down luminosity if the spin-down energy is accumulated and instantaneously released. However, unless there are materials with effective inertia such as supernova fallback disk, (e.g., Michel 1988), the spin-down energy would not

Lyutikov 2017). Taking into account the beaming fraction f_Ω to the intrinsic luminosity, the condition on the spin-down luminosity is

$$L_{\text{sd}} > f_\Omega L_{\text{FRB}}, \quad (1)$$

where L_{FRB} is the observed isotropic FRB luminosity. For the spin-down formula, we assume

$$L_{\text{sd}} \sim L_{\text{sd},i} \left(1 + \frac{t}{t_{\text{sd}}}\right)^{\frac{1+n}{1-n}}, \quad (2)$$

where t is an age of an NS, n is braking index of the rotation period, $\dot{P} \propto P^{2-n}$ (Manchester et al. 1985). The initial spin-down luminosity $L_{\text{sd},i}$ and the spin-down timescale t_{sd} are described by

$$L_{\text{sd},i} \sim \frac{B_{\text{d}}^2 (2\pi/P_i)^4 R_{\text{ns}}^6}{2c^3}, \quad (3)$$

and

$$t_{\text{sd}} \sim \frac{E_{\text{rot},i}}{L_{\text{sd},i}}, \quad (4)$$

where c is the speed of light, P_i is the initial period, B_{d} is the strength of the surface dipole magnetic field, and $E_{\text{rot},i}$ is the initial rotational energy of an NS,

$$E_{\text{rot},i} \sim \frac{1}{2} I \left(\frac{2\pi}{P_i}\right)^2. \quad (5)$$

The strongest observed burst in FRB 121102 (burst number 2 in Marcote et al. 2017) gives the most stringent constraint on L_{sd} . We use the burst with an isotropic luminosity of $L_{\text{FRB}} \sim 6 \times 10^{42} \text{ erg s}^{-1}$ (Marcote et al. 2017) detected at ~ 4 yr after the first burst detection.

Second, the pulse width w_{p} has to be shorter than the rotational period P for GRP-like emission. If the emission pattern is beamed, the pulse width relative to the rotation period should be short compared with the isotropic emission case. Using the beaming fraction f_Ω for a circular cone geometry, the condition on the rotation period is

$$P > f_\Omega^{-1/2} w_{\text{p}}, \quad (6)$$

unless all three axes, magnetic axis, rotation axis, and line-of-sight are nearly aligned. The temporal evolution of the rotation period is described by

$$P \sim P_i \left(1 + \frac{t}{t_{\text{sd}}}\right)^{\frac{1}{n-1}}. \quad (7)$$

The observed Gaussian FWHM is 2.8 – 8.7 ms for 17 bursts (Spitler et al. 2014; Spitler et al. 2016; Scholz et al. 2016). Although the widest observed pulse width was 8.7 ms for burst number 5 in Spitler et al. (2016), this pulse seems to be split into two components. Here, we adopt the second

be accumulated (Lyutikov 2017). Here, we do not consider such materials near the NS.

widest width 8.0 ms for burst number 10 in Spitler et al. (2016), though the following results would be almost comparable. Note that the width in the source rest frame is $(1+z)^{-1}$ times shorter than the observed one.

Figure 1 shows the constraints on the NS parameters P_i and B_d obtained from two conditions (1) and (6). Each panel shows the case with different parameter sets (f_Ω, n, t) . Since the first burst of FRB 121102 were detected in 2012 (Spitler et al. 2014), the NS age at which the strongest burst were detected (Marcote et al. 2017) is $t \gtrsim 4/(1+z)$ yr ~ 3.3 yr in the source rest frame. Figure 1 (A) shows the fiducial case with isotropic emission ($f_\Omega = 1$), dipole spin-down formula ($n = 3$), and the lower bound of the NS age $t = 3.3$ yr. Allowed ranges of parameters are very limited, $B_d \sim 10^{13}$ G and $P_i \lesssim 3$ ms. Such an NS with short P_i is very rare from the initial period distribution obtained by pulsar population studies (Faucher-Giguère & Kaspi 2006; Perera et al. 2013), the associated supernova remnants (Popov & Turolla 2012), and the total injected energy of pulsar wind nebulae (PWNe; Tanaka & Takahara 2013). The observed FRB luminosity is almost comparable to the spin-down luminosity in the allowed parameter region at $t = 3.3$ yr. Then, the observed FRB flux density at 1.4GHz will rapidly decay toward $\lesssim 1$ Jy because the NS age in the allowed region is already $t \gg t_{sd}$.

Figure 1 (B) shows the allowed parameter region in the anisotropic emission case, $f_\Omega = 0.1$. Since the intrinsic FRB luminosity is lower than the isotropic case, the allowed parameter region from the luminosity condition (1) becomes larger than the fiducial case (figure 1 (A)). The upper limit on the magnetic field is $B_d \sim 4 \times 10^{13}$ G. The fraction w_p/P should also reduce in the anisotropic emission case, so that the lower limit on the magnetic field becomes high at $t > t_{sd}$ compared with the fiducial case. As a result, the allowed range of the magnetic field is very limited, which is similar to the fiducial case. The allowed range of the initial period becomes large, $P_i \lesssim 10$ ms.

The braking index n is lower than that from the dipole spin-down formula ($n = 3$) in most young pulsars (e.g., Espinoza et al. 2017). Figure 1 (C) shows the NS parameter region in the low braking index case, $n = 2$. In the region $t \ll t_{sd}$, since conditions (1) and (6) do not depend on n (see equations 2 and 7), there is no allowed parameter region as the same as the case with $n = 3$. The allowed range of the initial period is $P_i \lesssim 2$ ms. The allowed magnetic field depends on P_i and becomes low for short P_i .

The upper limit on the magnetic field $B_{d,max}$ obtained from condition (1) is $B_{d,max} \propto (f_\Omega L_{FRB})^{\frac{1-n}{4}} t^{-\frac{n+1}{4}} P_i^{\frac{3-n}{2}}$. On the other hand, the lower limit on the magnetic field $B_{d,min}$ at $t \gg t_{sd}$ derived from condition (6) is $B_{d,min} \propto f_\Omega^{\frac{1-n}{4}} w_p^{\frac{n-1}{2}} t^{-\frac{1}{2}} P_i^{\frac{3-n}{2}}$. From the two constraints on the dipole magnetic field, we obtain the constraint on the age of the NS t in the source rest frame, described by

$$t < \frac{1}{2} I L_{FRB}^{-1} \left(\frac{w_p}{2\pi} \right)^{-2}$$

$$< 3.3 \left(\frac{L_{\text{FRB}}}{6 \times 10^{42} \text{ erg s}^{-1}} \right)^{-1} \left(\frac{w_p(1+z)}{8 \text{ ms}} \right)^{-2} \text{ yr.} \quad (8)$$

Note that there is no allowed parameter region at $t \ll t_{\text{sd}}$ if condition (8) are not satisfied. At $t = 8/(1+z) \text{ yr} \sim 6.7 \text{ yr}$, GRP-like emission model cannot explain the observations as shown in figure 1 (D). The upper limit on the age (inequality 8) does not depend on the beaming fraction f_Ω and the braking index n . Therefore, if the origin of FRB 121102 is the GRP-like emission from a very young NS, the NS was born in a short time before the first detection at 2012 and FRB signal with flux density $\gtrsim 1 \text{ Jy}$ will not be able to be detected after 2017.

3 DISCUSSION

We investigate the GRP-like emission model with circular cone emission geometry for an origin of repeating FRB 121102 to give constraints on the NS parameters from the observations. In addition to the luminosity condition that (a) the intrinsic luminosity of FRBs is lower than the spin-down luminosity as already discussed in some authors (e.g., Lyutikov 2017), we consider that (b) the intrinsic pulse width of FRBs is shorter than the rotational period. Condition (b) significantly reduces the allowed region of the NS parameters limited by only condition (a) as shown in Fig. 1. Since the constraints are drawn from the properties of the burst only, the results do not depend on the properties of the persistent source and the circumburst environment discussed in other papers (Metzger et al. 2017; Lyutikov 2017; Kashiyama & Murase 2017; Cao et al. 2017; Dai et al. 2017). The determined parameters within narrow region are the dipole magnetic field $B_d \sim 10^{13} \text{ G}$, and the initial period $P_i \lesssim 3 \text{ ms}$, if the emission is isotropically emitted ($f_\Omega \sim 1$) and temporal evolution follows the dipole radiation formula ($n = 3$). The allowed dipole magnetic field becomes high for the anisotropic emission case ($f_\Omega < 1$), and low for small braking index ($n < 3$), although the allowed range $\log(B_{d,\text{max}}/B_{d,\text{min}})$ does not depend on f_Ω and n , as shown in Figure 1. The maximum initial period becomes long for the anisotropic emission case, $P_{i,\text{max}} \propto f_\Omega^{-1/2}$.

The FRB luminosity is comparable to the spin-down luminosity, $f_\Omega L_{\text{FRB}} \sim L_{\text{sd}}$, for the NS in the allowed region of Figure 1. Although the radio efficiency required from the GRP-like model is higher than that of the observed Crab GRP ($\lesssim 0.01$), such a high efficiency is seen in coherent magnetospheric radio emission from some old pulsars which reside close to the death line in $P-\dot{P}$ plane (Szary et al. 2014). A high efficiency state may change a spin-down behavior coincidence at FRBs. A suggestive switching behavior of the spin-down and radio emission has been reported from Galactic intermittent pulsars (e.g., Kramer et al. 2006), which mechanism is proposed to be related

with the changes of the dissipation rate of the electromagnetic energy in the magnetosphere (e.g., Li et al. 2012). Furthermore, the required efficiency is reduced by other parameters. For example, if an NS is significantly massive, the moment of inertia could be a factor of a few times larger than our adopted value. Then, the ratio B_{\max}/B_{\min} could be high (from equation 8) and the required minimum efficiency could become an order of ~ 0.1 .

Anisotropic emission case has been discussed by Katz (2017a). In their extremely narrow, wandering beam model, the allowed parameter region for P and B_d is much large. However, they have not considered the lower limit on the rotation period from the FRB pulse width. For the circular cone emission geometry as usually considered in the pulsar radio emission (e.g., Rankin 1993), conditions (a) and (b) give significant constraints on the pulsar parameters (Figure 1). In addition, the constraint on the age (equation 8) does not depend on the beaming fraction f_Ω .

The observed flux of repulsive bursts from FRB 121102 has not shown apparent temporal evolution since the first detection (Spitler et al. 2014; Spitler et al. 2016; Scholz et al. 2016; Chatterjee et al. 2017; Marcote et al. 2017). On the other hand, the spin-down luminosity is expected to already decay as $L_{\text{sd}} \propto t^{\frac{1+n}{1-n}}$ at $t \sim 3.3$ yr (i.e., the allowed region in figure 1 satisfies at $t = 3.3 \text{ yr} > t_{\text{sd}}$). If the radio efficiency, $L_{\text{FRB}}/L_{\text{sd}}$, is constant, such behaviors are inconsistent. Note that the radio efficiency of GRP has been poorly understood (Eilek & Hankins 2016). The radio efficiency of normal pulse increases as the spin-down luminosity decreases in Galactic pulsars whose ages are older than the spin-down timescale (Szary et al. 2014). If the radio efficiency of GRP (and FRB) has the similar to that of normal pulse, the flux may show no apparent temporal evolution until $t \sim 3.3$ yr. However, once the radio efficiency reaches to the maximum value ~ 1 at the age $t \sim 3.3$ yr which does not depend on f_Ω and n (inequality 8), the observed radio flux density will rapidly decay ($\lesssim 1$ Jy) as the evolution of the spin-down luminosity even if the radio efficiency keeps nearly maximum at $t > 3.3$ yr. If FRBs with flux $\gtrsim 1$ Jy will be detected from repeating FRB 121102 after 2017 (i.e., $t > 3.3$ yr), we need to consider an alternative model, such as the magnetically powered flare from a magnetar (e.g., Popov & Postnov 2010; Lyubarsky 2014; Katz 2016a). Note that condition (6) is also working if the FRB emission occurs in the magnetar magnetosphere for the magnetically powered flare model.

Some other FRBs have comparable and wider observed pulse width (e.g., $w_p \sim 15.62$ ms for FRB 130729; Champion et al. 2016). However, after accounting for all instrumental and measurable propagation effects, the width of other all FRBs is smaller than ~ 3 ms (Scholz et al. 2016). Then, if other FRBs are also GRP-like emission and have similar luminosity $L \sim 10^{42} - 10^{43} \text{ erg s}^{-1}$, the activity timescale is $\lesssim 30 - 300$ yr, much longer than that of FRB 121102.

3.1 Uncertainties of Pulse Width

The observed pulse width would be broadened as results from multi-path propagation delay (e.g., Lee & Jokipii 1975; Rickett 1977). Then, the intrinsic pulse width of FRB would be overestimated. The scattering time in intergalactic medium is much shorter than the pulse width (Macquart & Koay 2013). Using the scattering time-DM trend in Galactic pulsars (Lorimer et al. 2013b; Cordes et al. 2016), the scattering time in the Galaxy is $\sim 0.1 - 0.2$ ms, which is much shorter than the time-resolution of the measurements after de-dispersion (Spitler et al. 2014). The contribution of the host galaxy to the scattering time is unknown. The detected angular broadening of the bursts and persistent radio source is similar to the expected our Galaxy scattering contribution (Marcote et al. 2017). If the scattering time-DM trend in the host galaxy is also similar to that of the Galaxy, from the DM in host galaxy, $55 \text{ cm}^{-3} \text{ pc} \lesssim \text{DM} \lesssim 255 \text{ cm}^{-3} \text{ pc}$ (Tendulkar et al. 2017), the scattering time is $10^{-3} - 0.9$ ms. Observationally, no evidence of the scatter broadening was seen in all bursts of FRB 121102 (Spitler et al. 2014; Spitler et al. 2016; Scholz et al. 2016). The upper limit on the observed scatter broadening for first burst is < 1.5 ms (Spitler et al. 2014). The conservative upper limit on the scatter broadening is the minimum pulse width among the observed bursts, 2.8 ms observed for burst number 6 in Spitler et al. (2016). Even if we adopt the pulse width $w_p = (8.0 - 2.8)/(1 + z)$ ms ~ 4.4 ms as the upper limit on the rotational period, the upper limit on the age (inequality 8) is $t \lesssim 7.8$ yr, only a factor of ~ 2 larger than that in no scatter broadening case. Note that although the observed pulse width has broad range, 2.8-8.7 ms (Spitler et al. 2016), this feature have also been seen in GRPs from the Crab pulsar (e.g., Mikami et al. 2016).

The time resolution after de-dispersion of FRB 121102 pulses is ~ 1 ms (Spitler et al. 2014; Katz 2016b). Even if the light curves were analyzed in higher time resolution, the scattering time with ~ 1 ms could be possible in current observational constraints (Spitler et al. 2014). Then, the pulsation structure could be washed out if the rotation period of the NS is $P \lesssim 1$ ms. The radio burst-like phenomena which continue up to ~ 10 rotation periods have been known in some pulsars (e.g., Lorimer et al. 2013a). The minimum period of an NS is $\sim 0.3 - 0.7$ ms which depends on the nuclear equation of state (e.g., Haensel et al. 1999). If the source of FRB 121102 is the sub-millisecond pulsar, the allowed range of the dipole magnetic field is $10^{11} \text{ G} \lesssim B_d \lesssim 10^{13} \text{ G}$ for the age $t = 3.3$ yr. Since the spin-down timescale becomes long for the NS with the low magnetic field and short rotation period, older NS age compared with the NS with long period ($P \gtrsim 1$ ms) could be possible to explain the observations. The upper limit on the age is $t \lesssim 100$ yr for the pulse width $w_p \sim 1$ ms. The detail periodicity search in a burst (e.g., Katz 2017a) and more stringent limit on the scatter broadening would be important to distinguish which range of period, $P \lesssim 1$ ms or $P \gtrsim 8$ ms, is appropriate as the source of FRB 121102.

3.2 Comparisons with Other Constraints

Observed DM and its time-derivative could give significant constraints on the origin of the FRB (e.g., Piro 2016; Metzger et al. 2017; Lyutikov 2017; Kashiyama & Murase 2017; Cao et al. 2017). Since an NS is formed as a result of core-collapse supernova, a young NS is generally surrounded by the dense ejecta. For simplicity, a DM through the ejecta may be described by $DM_{\text{ej}} \sim 3f_{\text{ion}}M_{\text{ej}}/(8\pi v_{\text{ej}}^2 t^2 m_{\text{p}})$, where M_{ej} and v_{ej} are the mass and velocity of the ejecta which mainly consist of α -elements, f_{ion} is the ionization fraction, and m_{p} is a proton mass. We assume singly ionization state for elements with the mean atomic mass number ~ 10 , so that $f_{\text{ion}} \sim 0.1$. An NS which resides the allowed range in figure 1 has a huge initial rotation energy $E_{\text{rot},i} \sim 3 \times 10^{52} (P_i/1\text{ms})^{-2}$ erg compared with a conventional supernova explosion energy ($\sim 10^{51}$ erg). Since the age in the allowed region is $t \gg t_{\text{sd}}$, the significant fraction of the rotation energy would be converted to the ejecta kinetic energy, $v_{\text{ej}} \sim \sqrt{2E_{\text{rot},i}/M_{\text{ej}}}$. Using the constraints $|dDM_{\text{ej}}/dt| \lesssim 2 \text{ cm}^{-3} \text{ pc yr}^{-1}$ for FRB 121102 estimated by Piro (2016), the maximum ejecta mass is estimated as $(M_{\text{ej}}/M_{\odot}) \lesssim 0.08(t/1\text{yr})^{3/2}(P_i/1\text{ms})^{-1}$. Then, for GRP-like model, the NS would be formed with low mass ejecta such as ultra-stripped supernova ($M_{\text{ej}} \sim 10^{-1}M_{\odot}$; e.g., Kleiser & Kasen 2014), accretion-induced collapse ($M_{\text{ej}} \sim 10^{-3}M_{\odot}$; e.g., Dessart et al. 2006), and binary NS merger ($M_{\text{ej}} \sim 10^{-4} - 10^{-2}M_{\odot}$; e.g., Hotokezaka et al. 2013), compared with conventional core-collapse supernova ($M_{\text{ej}} \sim 1 - 10M_{\odot}$).

The persistent radio emission also gives the significant constraints on the NS age if the persistent source is the emission from the PWN (e.g., Murase et al. 2016). Kashiyama & Murase (2017) showed that for the ejecta mass $\sim 0.1M_{\odot}$, the persistent source could be consistent with a PWN powered by an NS with our fiducial parameter sets, the dipole magnetic field $B_{\text{d}} \sim 10^{13}$ G, the initial rotation period $P_i \sim 1$ ms, and the age $t \sim 4$ yr. The range is consistent with our results from the observed FRB properties.

Acknowledgments

We are grateful to the anonymous referee for helpful comments. We would like to thank Y. Ohira, S. J. Tanaka, T. Terasawa and R. Yamazaki for fruitful discussions. This work was supported by KAKENHI 16J06773 (S.K.), 15H00845, 16H02198 (T.E.) and 25400221 (S.S.).

References

- Cao, X.-F., Yu, Y.-W., & Dai, Z.-G. 2017, ApJL, 839, L20
Champion, D. J., Petroff, E., Kramer, M., et al. 2016, MNRAS, 460, L30
Chatterjee, S., Law, C. J., Wharton, R. S., et al. 2017, Nature, 541, 58

Cheng, K. S., Ho, C., & Ruderman, M. 1986, *ApJ*, 300, 522

Cordes, J. M., & Wasserman, I. 2016, *MNRAS*, 457, 232

Cordes, J. M., Wharton, R. S., Spitler, L. G., Chatterjee, S., & Wasserman, I. 2016, arXiv:1605.05890

Dai, Z. G., Wang, J. S., & Yu, Y. W. 2017, *ApJL*, 838, L7

Daugherty, J. K., & Harding, A. K. 1982, *ApJ*, 252, 337

Dessart, L., Burrows, A., Ott, C. D., Livne, E., Yoon, S.-C., & Langer, N. 2006, *ApJ*, 644, 1063

Eilek, J. A., & Hankins, T. H. 2016, *JPIPh*, 82, 635820302

Espinoza, C. M., Lyne, A. G., & Stappers, B. W. 2017, *MNRAS*, 466, 147

Faucher-Giguère, C.-A., & Kaspi, V. M. 2006, *ApJ*, 643, 332

Goldreich, P., & Reisenegger, A. 1992, *ApJ*, 395, 250

Haensel, P., Lasota, J. P., & Zdunik, J. L. 1999, *A&A*, 344, 151

Hotokezaka, K., Kiuchi, K., Kyutoku, K., Okawa, H., Sekiguchi, Y., Shibata, M., & Taniguchi, K. 2013, *PhRvD*, 87, 024001

Karuppusamy, R., Stappers, B. W., & van Straten W. 2010, *A&A*, 515, 36

Kashiyama, K., & Murase, K. 2017, *ApJL*, 839, L3

Katz, J. I. 2016a, *MPLA*, 31, 1630013

Katz, J. I. 2016b, *ApJ*, 818, 19

Katz, J. I. 2017a, *MNRAS*, 467, L96

Katz, J. I. 2017b, *MNRAS*, 469, L39

Kirk, J. G., Skiæraasen, O. & Gallant, Y. A. 2002, *A&A*, 388, L29

Kleiser, I. K. W., & Kasen, D. 2014, *MNRAS*, 438, 318

Kramer, M., Lyne, A. G., O'Brien, J. T., Jordan, C. A., & Lorimer, D. R. 2006, *Science*, 312, 549

Lee, L. C., & Jokipii, J. R. 1975, *ApJ*, 201, 532

Li, J., Spitkovsky, A., & Tchekhovskoy, A. 2012, *ApJL*, 746, L24

Lorimer, D. R., Bailes, M., McLaughlin, M. A., Narkevic, D. J., & Crawford, F. 2007, *Science*, 318, 777

Lorimer, D. R., Camilo, F., & McLaughlin, M. A. 2013a, *MNRAS*, 434, 347

Lorimer, D. R., Karastergiou, A., McLaughlin, M. A., & Johnston, S. 2013b, *MNRAS*, 436, L5

Lyubarsky, Y. 2014, *MNRAS*, 442, L9

Lyutikov, M., Burzawa, L. & Popov. S. B., 2016, *MNRAS*, 462, 941

Lyutikov, M. 2017, *ApJL*, 838, L13

Macquart, J.-P., & Koay, J. Y. 2013, *ApJ*, 776, 125

Marcote, B., Paragi, Z., Hessels, J. W. T., et al. 2017, *ApJL*, 834, L8

Manchester, R. N., Newton, L. M., & Durdin, J. M. 1985, *Nature*, 313, 374

Metzger, B. D., Berger, E., & Margalit, B. 2017, *ApJ*, 841, 14

Mikami, R., Asano, K., Tanaka, S. J., et al. 2016, *ApJ*, 832, 212

Michel, F. C. 1988, *Nature*, 333, 644

Murase, K., Kashiyama, K., & Mészáros, P. 2016, *MNRAS*, 461, 1498

Park, S., Yang, J., Oonk, J. B. R., & Paragi, Z. 2017, *MNRAS*, 465, 3943

Perera, B. B. P., McLaughlin, M. A., Cordes, J. M., Kerr, M., Burnett, T. H., & Harding, A. K. 2013, *ApJ*, 776, 61

Piro, A. L. 2016, *ApJL*, 824, L32

Popov, S. B., & Postnov, K. A. 2010, in *Proc. of Conf. Dedicated to Viktor Ambartsumian's 100th Anniversary, Evolution of Cosmic Objects Through Their Physical Activity*, Vol. 129, ed. H. A. Harutyunian, A. M. Mickaelian, & Y. Terzian (Yerevan: NASRA), 129

Popov, S. B., & Turolla, R. 2012, *Ap&SS*, 341, 457

Rankin, J. 1993, *ApJ*, 405, 285

Rickett, B. J. 1977, *ARA&A*, 15, 479

Spitler, L. G., Cordes, J. M., Hessels, J. W. T., et al. 2014, *ApJ*, 790, 101

Spitler, L. G., Scholz, P., Hessels, J. W. T., et al. 2016, *Nature*, 531, 202

Scholz, P., Spitler, L. G., Hessels, J. W. T., et al. 2016, *ApJ*, 833, 177

Szary, A., Zhang, B., Melikidze, G. I., Gil, J., & Xu, R.-X. 2014, *ApJ*, 784, 59

Tanaka, S. J., & Takahara, F. 2013, *MNRAS*, 429, 2945

Tendulkar, S. P., Bassa, C. G., Cordes, J. M., et al. 2017, *ApJL*, 834, L7

Tendulkar, S. P., Kaspi, V. M., & Patel, C. 2016, *ApJ*, 827, 59

Thornton, D., Stappers, B., Bailes, M., et al. 2013, *Science*, 341, 53